

Preliminary Assessment of Flying and Handling Qualities for mini-UAVs

Original

Preliminary Assessment of Flying and Handling Qualities for mini-UAVs / Capello, Elisa; Guglieri, Giorgio; Marguerettaz, Paolo; Quagliotti, Fulvia. - In: JOURNAL OF INTELLIGENT & ROBOTIC SYSTEMS. - ISSN 0921-0296. - STAMPA. - 65:1-4(2012), pp. 43-61. [10.1007/s10846-011-9565-5]

Availability:

This version is available at: 11583/2466580 since:

Publisher:

Springer

Published

DOI:10.1007/s10846-011-9565-5

Terms of use:

This article is made available under terms and conditions as specified in the corresponding bibliographic description in the repository

Publisher copyright

(Article begins on next page)

Preliminary assessment of flying and handling qualities for mini-UAVs

Elisa Capello · Giorgio Guglieri ·
Paolo Marguerettaz · Fulvia Quagliotti

Abstract The purpose of this work is to identify some criteria for the evaluation of flying and handling qualities of small scale Unmanned Aerial Vehicles (mini-UAVs). A possible solution for the evaluation of handling qualities is based on the minimization of cumulative cross track error (estimated along a sequence of waypoints) at constant altitude and speed, assuming gradual variation of the control inputs (throttle, elevator and ailerons). A complete parametric analysis of vehicle open loop dynamics is performed for a demonstrative mini-UAV. The flying and handling qualities are assessed implementing the selected platform in a full state flight simulator including a realistic autonomous navigation and control system. Different target paths are considered and a parametric study based on the minimization of the cross track error is presented. A section of conclusions summarizes the key results and presents suggestions for future work.

Keywords Flying qualities · Handling qualities · UAV · Modeling and simulation

Nomenclature and Acronyms

| | |
|--------------|---|
| b | Wing span [m] |
| n/α | Load factor derivative [g/rad] |
| $C_{l\beta}$ | Lateral stability derivative [-] |
| $C_{n\beta}$ | Directional stability derivative [-] |
| h | Altitude [m] |
| I_X | Moment of inertia along X body axis [kgm ²] |
| I_Y | Moment of inertia along Y body axis [kgm ²] |
| n | Load factor [-] |
| V | Airspeed [m/s] |
| α | Angle of attack [rad] |
| ζ | Damping ratio [-] |
| τ_R | Roll time constant [s] |
| ω_n | Natural frequency [rad/s] |
| CT | Cross track error |
| DR | Dutch roll mode |
| FQ | Flying Qualities |
| HQ | Handling Qualities |
| PH | Phugoid mode |
| RPV | Remote Piloted Vehicle |
| SP | Short period mode |
| UAV | Unmanned Aerial Vehicle |

E. Capello (✉) · G. Guglieri · P. Marguerettaz ·
F. Quagliotti
Dipartimento di Ingegneria Aeronautica e Spaziale,
Politecnico di Torino, Turin, Italy
e-mail: elisa.capello@polito.it

1 Introduction

The purpose of this work is to identify some criteria for the evaluation of flying and handling

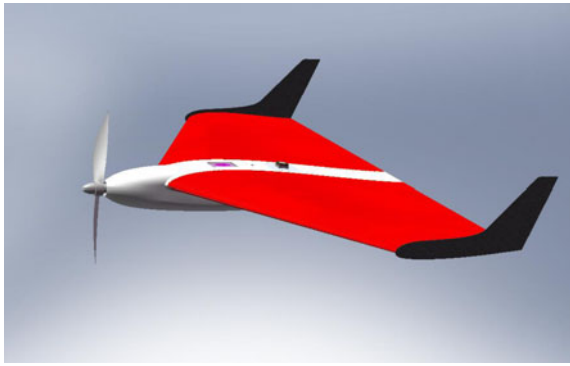


Fig. 1 MH850 mini-UAV configuration

qualities of small scale Unmanned Aerial Vehicles (UAVs). A novel method for the evaluation of handling qualities is based on the minimization of cumulative cross track error (estimated along a sequence of waypoints) at constant altitude and speed, assuming gradual variation of the control inputs (throttle, elevator and ailerons). The compliance of UAVs with response oriented flying qualities criteria is a prerequisite to successfully perform the planned mission. In previous works [2, 9] mission requirements are expressed in function of payload and ground control station characteristics, data link time delays and system failure modes. In this preliminary paper, the autonomous mode is analyzed, the interaction with the ground segment is not considered, and no considerations are made in terms of endurance and energy minimization. The objective of this approach is to verify if the designed platform can accomplish the planned mission, reducing the overall costs and flight tests time.

Table 1 List of the components (mass breakdown)

| Component | Weight [g] |
|---------------------|------------|
| Autopilot | 37.4 |
| GPS antenna | 11.2 |
| Battery | 272.6 |
| Autopilot battery | 28.9 |
| RC receiver | 15.6 |
| Transmitter | 15.7 |
| Transmitter antenna | 8.3 |
| Engine | 60.1 |
| Propeller | 30.1 |
| Regulator | 18.9 |

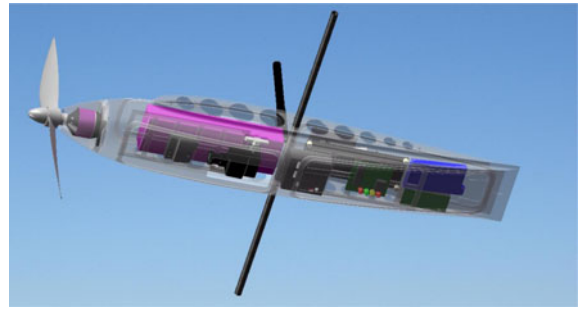


Fig. 2 The layout of the on-board components

Civil and military applications based on UAVs have been widely investigated and developed by aerospace industries and universities. The majority of current vehicle concepts rely on fixed wings, because they generally provide wider applications in terms of payload capabilities, ability to better withstand adverse weather conditions and flight performances, such as range and endurance. Fixed wing UAVs proved to be adequate for different types of missions, and the improvement of their performance is an important topic for present and future research.

One central theme in previous flying qualities documents [1, 6] is that aircraft performance is tailored to optimize the pilot–aircraft interaction. The standards used for FQ have not been updated to address UAV requirements and mission. UAV specifications do not consider changes in FQ due to sensor and payload requirements.

Table 2 The MH850 characteristics

| Geometric characteristics | |
|---|------------------------------------|
| Wing span | $b = 872$ mm |
| Aspect Ratio | $A = 3$ |
| Geometric sweep | $\Lambda = 25^\circ$ |
| Mass | 973 g |
| Propulsion | |
| Motor | Electric brushless (out-runner) |
| Maximum power | 200 W |
| Battery | 3400 mAh (3S1P LiPo) |
| Performance | |
| Maximum airspeed | $V > 20$ m/s (72 km/h) |
| Cruise airspeed | $V = 13.5$ m/s (48 km/h) |
| Endurance (cruise airspeed— $h = 100$ m) | > 70 min |

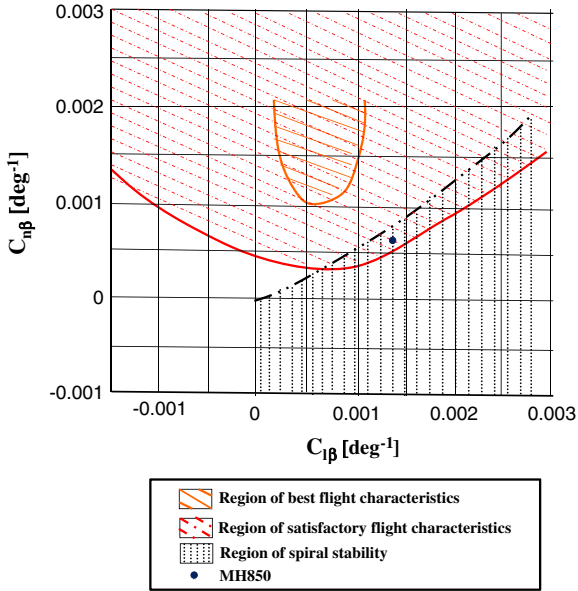


Fig. 3 Effects of variation of lateral and directional stability derivatives

Furthermore, some existing criteria cannot be applied “as is” to UAVs.

The first study on Remote Piloted Vehicles [3] has been carried out in the late 70’s to adapt military standards for manned aircraft to the growing number of unmanned vehicles. More recently, the attention was focused on the flying qualities of small scale UAVs, as in [17, 18]. Williams highlights the need to specify the flying and handling qualities using flight test techniques to overcome handling deficiencies in the early stages of flight control implementation. In particular, Williams’ works discuss the need to derive UAV standards taking into account the flight control system requirements. A later work defines flying criteria focused on a dynamic scaling approach [8]. Foster suggests that UAV short period natural frequency limits should be substantially revised if compared with those used for traditional aircraft.

As in [12], the first approach applied in this paper is the adaptation of open loop manned standards to small scale UAVs (response oriented vision). The second approach is based on the identification of new criteria focused on the mission requirements (task oriented vision). In this last case, the pilot is substituted by a flight control system (off the shelf autopilot) implemented in the

simulation of the autonomous missions (computer in command mode). The authors verify that an adequate mission oriented design is a key feature to obtain satisfactory flying handling qualities and [11, 16].

A test vehicle (mini-UAV) is presented in Section 2. A complete parametric analysis of vehicle open loop dynamics is performed. Section 3 outlines the FQ criteria for a generic fixed-wing mini-UAV. In Section 4, the handling qualities are assessed implementing the selected platform in a full state flight simulator including a realistic autonomous navigation and control system. Different target paths are considered and a demonstrative parametric study based on the minimization of the cross track error is presented. A section of conclusions summarizes the key results and presents suggestions for future work.

2 MH850 mini UAV

MH850 [14] is the last member of the MicroHawk line of mini-UAVs [10]. It has been developed for low cost alpine surveillance missions. High altitude, low temperature, strong winds, changeable weather conditions, rough terrain and lack of tactical support are the boundary conditions for this type of missions. The fuselage has a complex profiled shape. The swept wing has a moderate taper ratio (less than 900 mm wing span) without twist and dihedral. Aircraft control is obtained with trailing edge elevons (equivalent dual function as elevator δ_ϵ and aileron δ_α). MH850 has enough specific excess power to climb with non-

Table 3 MH850 longitudinal and lateral-directional modes

| | Natural frequency [rad/s] | Damping | Period [s] | Half time [s] |
|----------------------------|---------------------------|---------|------------|---------------|
| Longitudinal | | | | |
| Short period | 17.058 | 0.477 | 0.419 | 0.085 |
| Phugoid | 0.898 | 0.075 | 7.018 | 10.283 |
| Lateral-directional | | | | |
| Dutch roll | 6.145 | 0.125 | 1.030 | 0.898 |
| Roll mode | 14.255 | 1 | – | 0.048 |
| Spiral mode | 0.0002 | 1 | – | 69.240 |

Fig. 4 Natural frequencies as a function of flight altitude

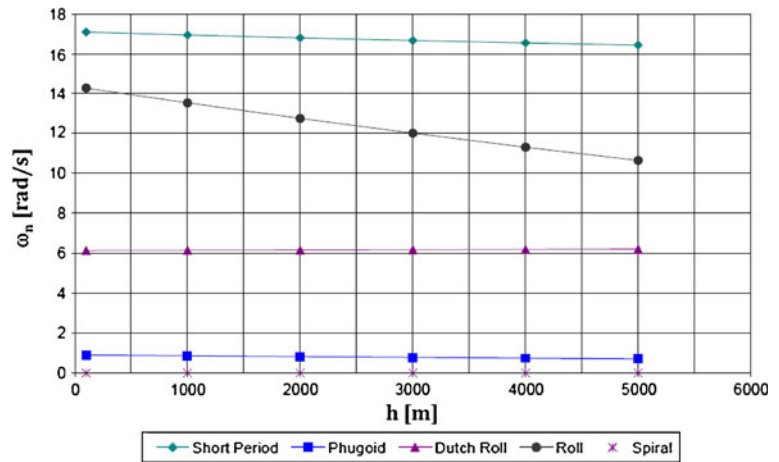


Fig. 5 Damping ratios as a function of flight altitude

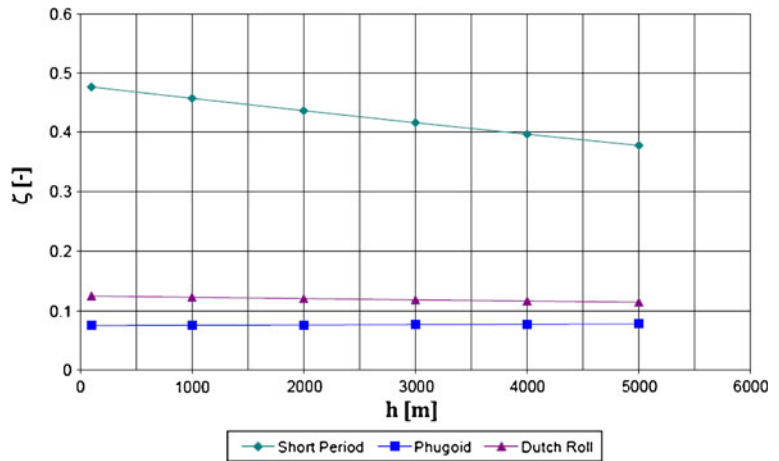


Fig. 6 Natural frequencies as a function of flight airspeed

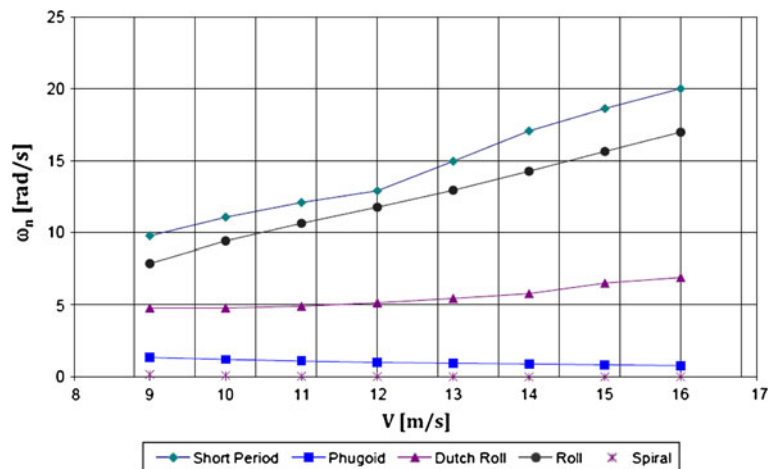
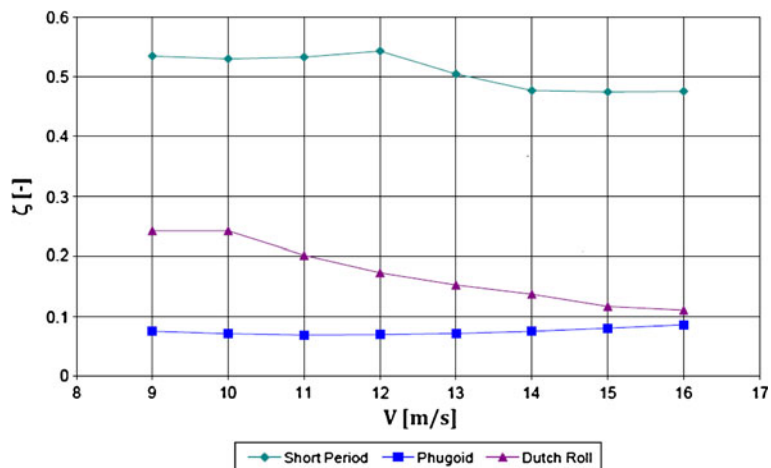


Fig. 7 Damping ratios as a function of flight airspeed



marginal rates at altitude. Only 45% of maximum power is required for level flight at sea level.

A nose cone covers the front mounted electric motor. Removable panels give rapid access to components and the substitution of battery packs is very simple and quick. Payload and autopilot are also readily accessible (Fig. 1, Table 1).

The material chosen for wing production is Expanded Poly-Propylene (EPP). This material is extremely light and provides adequate elastic behavior, it does not absorb moisture and it has an acceptable surface finish. Forming is obtained by simple hot wire cutting (a low cost manufacturing process). Due to EPP elasticity, moderate impacts do not leave dents on the outer contours of the vehicle. The fuselage is made of sintered nylon profiled with a rapid prototyping technique. Laser sintering enables complex shapes to be formed with precision at reasonable costs (assuming a limited number of samples). Internal volumes and aerodynamics can be also improved updating the design of the fuselage with a negligible increase in manufacturing costs. The position and the layout of on-board components have been assessed in order to balance the vehicle with an appropriate

Table 4 Damping ratio limits (phugoid mode)

| | |
|---------|---------------------------|
| Level 1 | Equivalent $\zeta > 0.04$ |
| Level 2 | Equivalent $\zeta > 0.00$ |
| Level 3 | $T_2 > 55$ seconds |

static margin (see Fig. 2). The most relevant features of MH850 are reported in Table 2.

The design of tailless aircraft must account for an adequate longitudinal static stability (tumbling longitudinal boundary) and sufficient control authority. Trailing edge elevons also induce a lift penalty due to the negative deflection required to trim that must be minimized [7]. Another typical drawback of all-wing aircraft is a marginal damping of Dutch roll oscillatory mode. Hence, vertical wingtip stabilizers must be designed as a compromise between dihedral effect ($C_{l\beta}$ derivative) while maintaining an acceptable directional stability ($C_{n\beta}$ derivative). The collateral effect may be limited spiral mode instability at higher airspeeds. Jones [13] studied the stability and control of tailless aircraft. For lateral directional stability he identified experimentally regions of good stability varying the lateral and directional derivatives (Fig. 3). As seen in Fig. 3 the value of the directional stability derivative $C_{n\beta}$ for tailless aircraft is usually smaller than 0.001 deg^{-1}

Table 5 Damping ratio limits (short period)

| Level | Category A and C | | Category B | |
|-------|----------------------|----------------------|----------------------|----------------------|
| | Minimum ζ_{SP} | Maximum ζ_{SP} | Minimum ζ_{SP} | Maximum ζ_{SP} |
| 1 | 0.35 | 1.30 | 0.30 | 2.00 |
| 2 | 0.25 | 2.00 | 0.2 | 2.00 |
| 3 | 0.15 | – | 0.15 | |

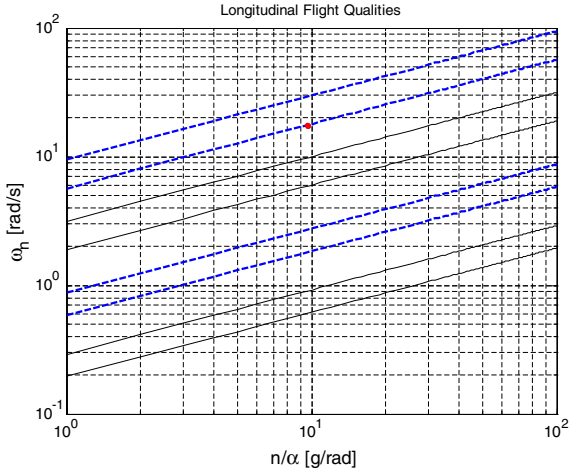


Fig. 8 Short period natural frequency limits (*solid line* MIL criteria, *dashed line* Foster's criteria)

(0.0575 rad^{-1}), falling outside of the region designated for best flight characteristics.

Considering the reference mini-UAV (MH850 in cruise flight), the directional derivative $C_{n\beta}$ is 0.037 rad^{-1} and the lateral derivative $C_{l\beta}$ is -0.078 rad^{-1} . Hence MH850 can be located within the region of satisfactory flight characteristics (for a nominal static margin of 7.5%), with a stable spiral mode.

A study of dynamic stability for MH850 has been also performed considering a decoupled lin-

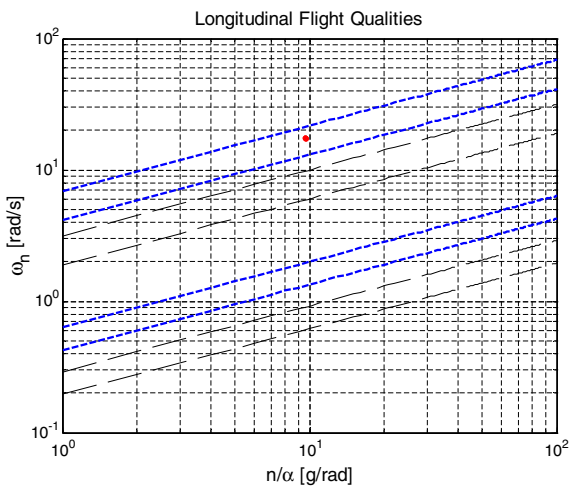


Fig. 9 Short period natural frequency limits (*dashed line* MIL criteria, *solid line* authors' criteria)

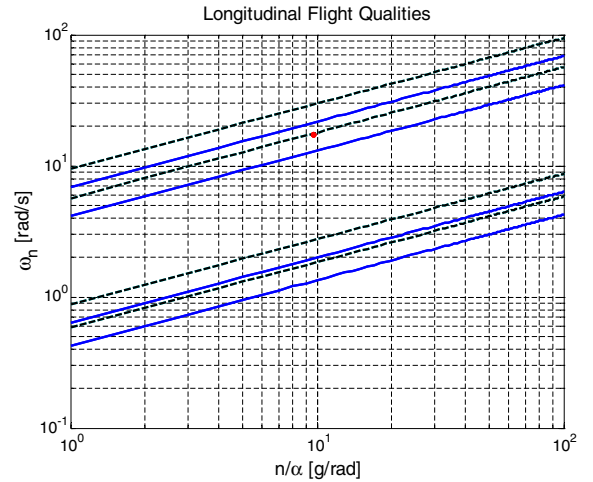


Fig. 10 Short period natural frequency limits (*dashed line* Foster's criteria, *solid line* present criteria)

ear model. The dynamic behaviors of large and small scale aircraft are described by similar modes, even if the small masses and moments of inertia of mini-UAVs produce higher natural frequencies. The characteristic dynamic modes have a major impact on aircraft FQs and many of the military specifications are derived by setting limits on the natural frequencies and damping ratios of the typical modes (phugoid, short period, Dutch roll, spiral and roll mode).

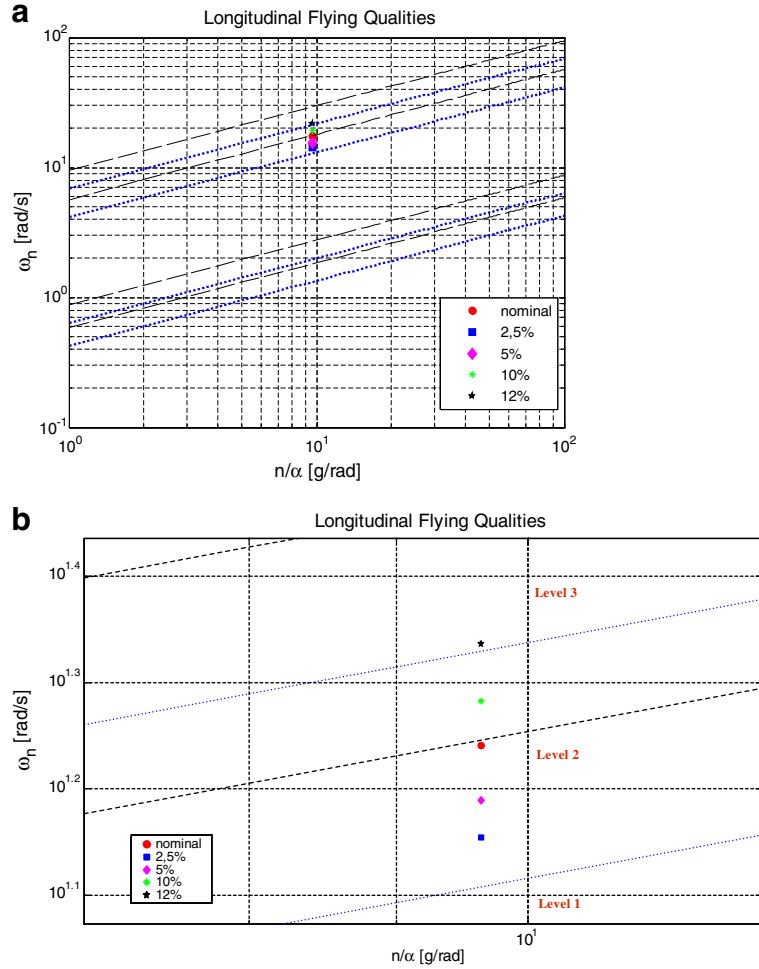
If the following state space system (only states and inputs) is considered

$$\begin{cases} X_{\text{long}} = \{u, w, q, \theta\}^T \\ X_{\text{lat}} = \{v, p, r, \varphi, \psi\}^T \\ U_{\text{long}} = \{\delta_{th}, \delta_e\}^T \\ U_{\text{lat}} = \{\delta_a\}^T \end{cases}$$

analyzing the cruise condition ($V = 13.5 \text{ m/s}$; $h = 100 \text{ m}$), all poles are stable and lie in the left half plane of root locus (as explained in Table 3).

By changing the flight altitude with constant dynamic pressure, as shown in Figs. 4 and 5, the variation of the natural modes characteristics is generally negligible. The only relevant variation can be noted for the roll mode: if the altitude is increased, the natural frequency is reduced up to 25% (if a maximum altitude of 5000 m is considered). The short period exhibits a reduction of its damping ratio of about 20% climbing from 100 m to 5000 m.

Fig. 11 Natural frequency of short period as a function of static margin: **a** complete visualization; **b** detailed visualization with Level definition. (The Levels refer to the scaling factor suggested by the authors)



By changing the flight airspeed (constant altitude $h = 100$ m), the overall modal response remains stable for the entire flight envelope, with the only exception of the spiral mode (marginal

instability). The short period and the roll mode natural frequencies sharply increase (100% approximately) at higher airspeeds while the damping ratio of the Dutch roll mode is reduced (60%).

Flight tests demonstrate good aircraft behavior across the entire flight envelope (Figs. 6 and 7).

Table 6 Limits for Dutch roll natural frequency and damping ratio

| Level | Flight phase category | Class | Min ζ_d | Min $\zeta_d \omega_d$ [rad/s] | Min ω_d [rad/s] |
|-------|-----------------------|-------------|---------------|--------------------------------|------------------------|
| 1 | A | I, IV | 0.19 | 0.35 | 1.00 |
| | | II, III | 0.19 | 0.35 | 0.4 |
| | B | All | 0.08 | 0.15 | 0.4 |
| 2 | All | I, II-C, IV | 0.08 | 0.15 | 1 |
| | | II-L, III | 0.08 | 0.15 | 0.4 |
| 3 | All | All | 0.02 | 0.05 | 0.4 |
| 3 | All | All | 0.02 | – | 0.4 |

Table 7 Limits of roll mode time constant

| Flight phase category | Class | Level | | |
|-----------------------|-------------|-------|-------|------|
| | | 1 | 2 | 3 |
| A | I, IV | 1.0 s | 1.4 s | 10 s |
| | II, III | 1.4 s | 3 s | |
| B | All | 1.4 s | 3 s | |
| C | I, II-C, IV | 1.0 s | 1.4 s | |
| | II-L, III | 1.4 s | 3.0 s | |

Table 8 Requirements for spiral mode time to double

| Class | Flight phase category | Level | | |
|----------|-----------------------|-------|------|-----|
| | | 1 | 2 | 3 |
| I, IV | A | 12 s | 12 s | 4 s |
| | B & C | 20 s | 12 s | 4 s |
| II & III | All | 20 s | 12 s | 4 s |

3 Flying Qualities Criteria

Flying qualities are “a set of properties that describe the ease and the effectiveness with which an aircraft responds to command inputs in function of the designed mission” [6]. Aircraft flying qualities design specifications are intended to enforce mission requirement and flight safety regardless of design implementation [2]. The requirements for manual and automatic flight control tend to differ. Many automatic control requirements are stated in terms of closed-loop performance or accuracy of a guidance or flight control parameter. Although performance is implied, FQ specifications for piloted aircraft are not stated in terms of the actual mission flight phase performance of the closed-loop pilot–vehicle combination. For unmanned platform, the criteria are related to the performance requirements, including operational characteristics, data link and ground control station.

Considering the classification presented in [3] the MH850 falls in Class I (small RPVs). In a similar way, the flight phases are combined into four categories. In our case, the selected category is B (gradual maneuver without precision tracking but accurate flight path control), taking into account the typical MH850 mission (surveillance and territorial monitoring on a target area with constant speed and altitude).

The system response is analyzed evaluating the flying qualities criteria separately for the two planes

Table 9 Reference flight parameters

| | | | |
|-------------------|--------------|------|--|
| Cruise airspeed | V = 13.5 m/s | | |
| Height | h = 100 m | | |
| Cruise throttle | 45% | | |
| Elevon deflection | min | −15° | |
| | max | +15° | |
| Static margin | min | 2.5% | |
| | max | 12% | |

(longitudinal and lateral-directional planes). As an additional note, statically and dynamically stable platforms enhance the effectiveness of surveillance missions as a result of damped vehicle’s response to turbulence (higher quality of video streams obtained with un-stabilized optical systems).

3.1 Longitudinal Criteria

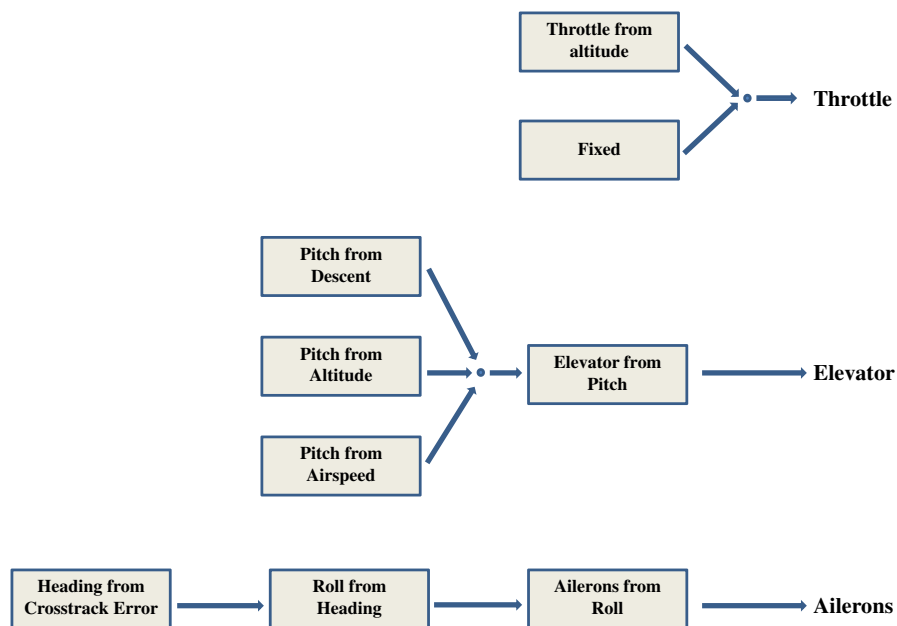
For the longitudinal plane, damping and natural frequencies of short period and phugoid mode are analyzed. For the phugoid case no limits are imposed on natural frequency. A Level 1 flight requires a positive and greater than 0.04 damping ratio. For the MH850 nominal case damping ζ_{PH} is equal to 0.07. The phugoid does not require other specifications because long period mode oscillations are slow with long half-time (according to the aircraft size; Table 4).

The short period mode influences the angle of attack and the flight-path angle. For this reason, the short period has to be fast enough and well damped to allow rapid maneuvers and trajectory changes. The damping ratio requirements for the short period are reported in Table 5. As indicated in Table 3 the damping ratio of MH850 for the short period is 0.48, thus a Level 1 flight is verified.

The natural frequency requirements are plotted against the load factor derivative n/α . As previously explained, the criteria adopted for piloted aircraft are not suitable for small scale UAVs, as evident in Fig. 8. Considering the standards, the reference vehicle exhibits a Level 3 flight, which means that its flying qualities should be quite unsatisfactory. Differently, flight tests demonstrate that Level 1 flight is shown for the complete range of flight conditions. This mismatch is due to the standard imposed FQ criteria. The military standards for piloted system are not revised for unmanned vehicles with higher short period natural frequencies. For this reason, in [8] a scaling factor (as a function of the wing span only) for the plot of Fig. 8 is proposed. The reference vehicle considered in Foster’s work is Boeing 747 and the scaling factor is $\frac{\omega_1}{\omega_0} = \sqrt{\frac{b_1}{b_0}} = \sqrt{80}$.

Using Foster’s scaling factor, the MH850 mini-UAV exhibits Level 1–2 flight, but the justification of this approach presented by Foster

Fig. 12 Autopilot functional scheme as implemented in the simulator



both in his master thesis and in [8] is not exhaustive enough. The authors propose a different scaling factor to adapt the standard limits for small scale UAVs. This proposed factor is

$$\frac{\omega_1}{\omega_0} = \frac{V_1 \bar{c}_1}{V_0 \bar{c}_0} \sqrt{\frac{b_1 I_{Y0}}{b_0 I_{Y1}}}$$

where ω is the natural frequency, V is the aircraft airspeed, b is the wing span and I_Y is the moment

of inertia along the Y body axis. The subscript 0 indicates the aircraft considered as reference and the subscript 1 the mini-UAV. If a Cessna 152 is considered as a reference, we obtain the results presented in Fig. 9. The Cessna is selected instead of Boeing 747 because the overall closer similarity with small scale UAVs. As evident, even if the scaling factor is designed taking into account geometric and physical characteristics, small scale unmanned vehicles present completely different

Fig. 13 The trend of the angle of pitch with different static margins (square pattern)

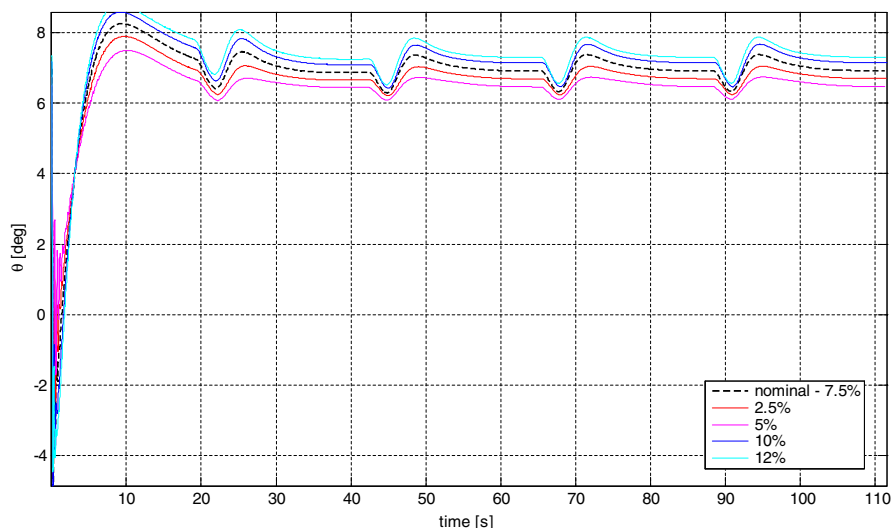
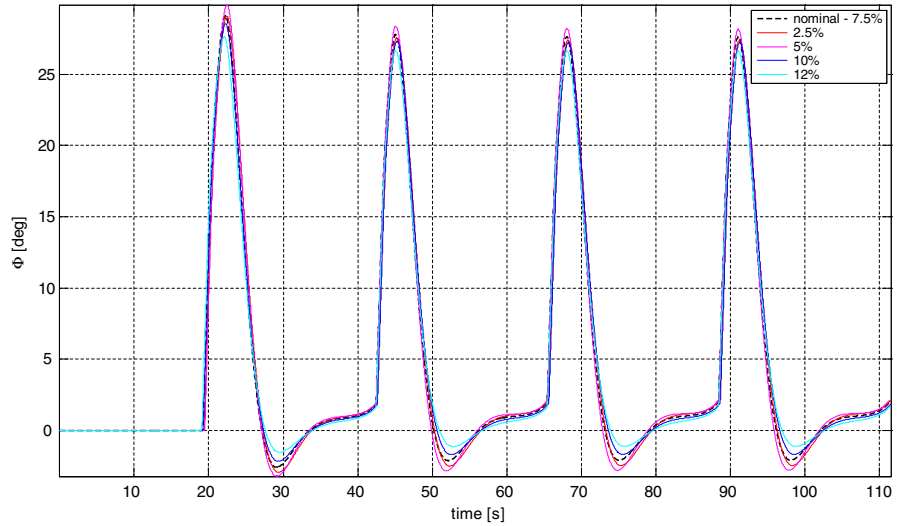


Fig. 14 The trend of the angle of roll with different static margins (square pattern)



features with respect to large piloted aircraft.¹ The lower frequency boundary should be probably shifted towards the higher appropriate ranges typical of mini-UAVs (Fig. 10).

The short period natural frequency and the control gradient n/α were estimated by varying the position of the on-board components i.e. by varying the static margin. The nominal static margin is 7.5% and due to the geometrical constraints of MH850 the minimum value is 2.5% and the maximum is 12%. The results are presented in Fig. 11. If the static margin is decreased (centre of gravity closer to the neutral point) the vehicle is characterized by Level 1 flight, which implies an improvement of the flying qualities over the nominal case. During flight tests the authors have verified an opposite result i.e. decreasing the static margin can degrade the flight behavior. These considerations demonstrate that both the proposed scaling factor and the MIL boundaries are not appropriate.

Future work should try to identify new regions of compliance with FQ levels by sampling existing mini-UAVs with different dimensions and weights, in order to determine the correct natural frequency domain, in accordance with the real flight characteristics verified by extensive flight test experiments.

¹Comparable results are obtained using the geometric and inertial characteristics of the Boeing 747.

3.2 Lateral Directional Criteria

Similar considerations apply for the lateral-directional plane. The lower limits are presented in Table 6 for the Dutch roll modal response (DR).

As indicated in Table 3, the DR natural frequency is 6.15 rad/s and the damping ratio is 0.125: thus the prescribed Level 1 limits are respected (MH850 mission is in Cat. B). This result is confirmed by the in-flight behavior of the real aircraft.

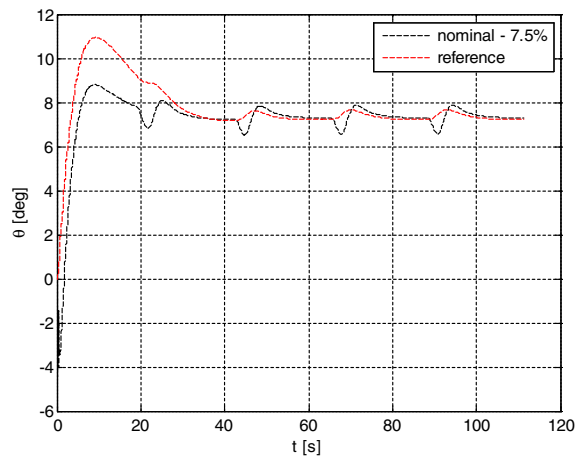


Fig. 15 The trend of the angle of pitch with the nominal static margin (square pattern)

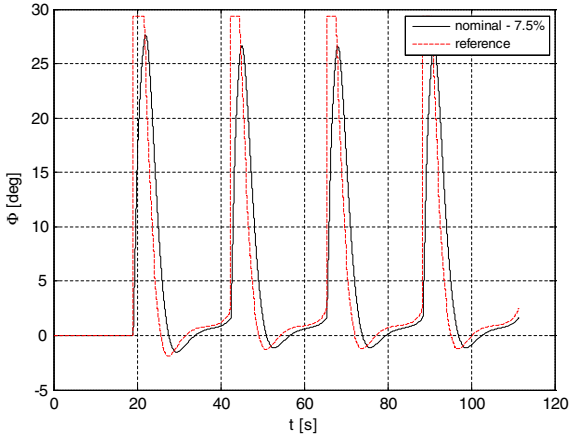


Fig. 16 The trend of the angle of roll with the nominal static margin (square pattern)

The constraints for non-oscillatory modes are considered through their time constants. The roll mode the time constant τ_R can be estimated as

$$\tau_R = -\frac{4I_X}{\rho S U_0 b^2 C_{lp}} = 0.069 \text{ s}$$

where I_X is the moment of inertia along the X axis, V is the airspeed, b is the wing span and C_{lp} is the rolling moment damping derivative. This constant has to be lower than the values indicated in Table 7. As for the other case, MH850 exhibits Level 1 flight (confirmed by flight experiments).

The spiral mode stability is analyzed considering also the aircraft class (this is not evaluated for the manned standards). In this case, the superposition of spiral stability and flight control-

Fig. 17 The trend of airspeed with different static margins (square pattern)

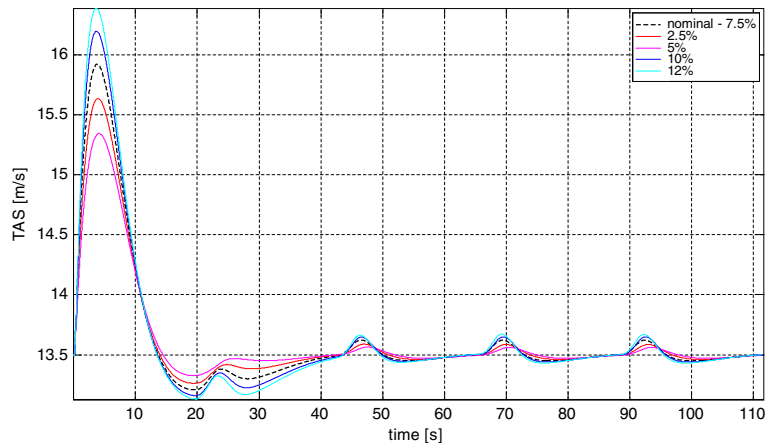


Table 10 Altitude offset limits as a function of the angle of bank

| Angle of bank | 0–1 deg | 1–30 deg | 30–60 deg |
|--------------------|-------------|-------------|-------------|
| Altitude variation | ± 30 ft | $\pm 0.3\%$ | $\pm 0.4\%$ |

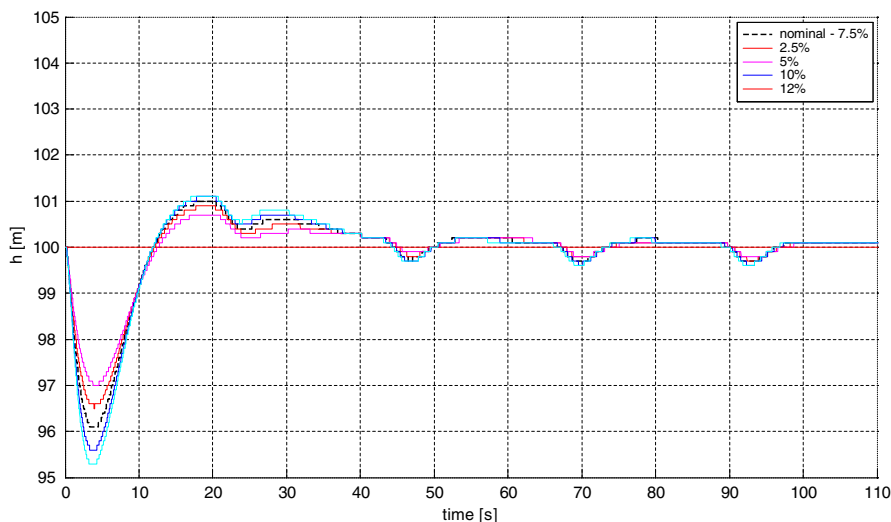
system characteristics shall be represented by the time to double (following a disturbance of up to 20 degrees). The time has to be greater than the reference values in Table 8.

4 Handling Qualities Criteria

To ensure that remote piloted and autonomous aircraft can perform their mission effectively and safely it is necessary to define a set of exhaustive requirements for the assessment of vehicle's handling qualities. In MIL-STD-1797A [1] handling qualities are “those qualities or characteristics of an aircraft that govern the ease and precision with which a pilot is able to perform the tasks ...”. As evident from this definition, some other factors have to be considered if the concept is extended to mini-UAVs. In [3] data link and control station requirements are introduced for remote piloted aircraft. Furthermore, the same reference clearly states that Level 1 rating for autonomous flight phases implies specific requirements for the dynamic stability of vehicle's attitude response (modal damping of the augmented aircraft).

As a matter of fact, the handling qualities of UAVs in general are those characteristics pertinent to vehicle's dynamics that allow precise

Fig. 18 The trend of altitude with different static margins (square pattern)



navigation and control with bounded command variations. This feature is verified if (a) the tracking error for attitudes and other flight parameters is limited (b) the cross track error is minimized i.e. the planned flight sequence is followed with accuracy with a bounded steering action of control inputs. A set of simulations was used to verify the handling qualities of MH850, following the above mentioned verification steps. The analysis is performed at the variation of the static margin because in operational environment the center of mass cannot be defined only with uncertainty. The simulation parameters are given in Table 9.

The simulations have been performed using a Fortran based software. The implemented autopilot is a commercial multi loop PID autopilot (Micropilot MP2028 or equivalent). Capabilities include attitude holding, airspeed holding, altitude

holding, turn coordination and sequential GPS waypoint navigation. The functional scheme of the PID loops is represented in Fig. 12. Flight control designs are usually based on PID controllers, since it is relatively straightforward to modify parameters in order to achieve the closed-loop specifications. The control gains and the simulator have been tested and experimentally validated using flight test data [4, 5]. The aircraft rigid body model is detailed in terms of propulsive, aerodynamic and inertial actions. The propulsion system is modeled as: propeller, DC motor and the batteries. Propeller aerodynamics is implemented using the blade element theory corrected for inflow effects. Blade airfoil aerodynamics is generated with a Reynolds number dependent database. The DC motor is parameterized with no-load and stall current, nominal voltage and stall torque.

Fig. 19 Simulation patterns (left square; right butterfly)

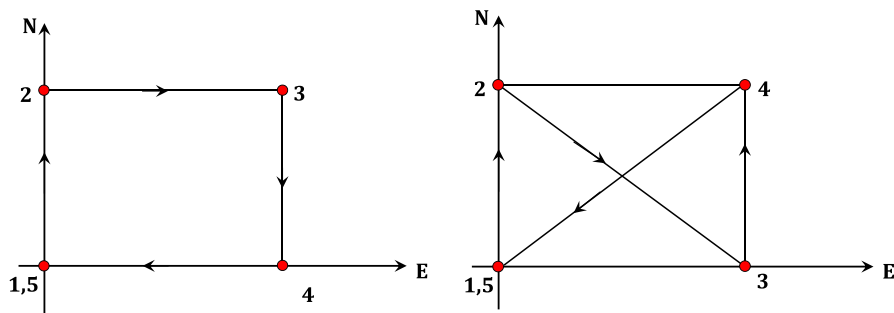


Table 11 Cumulative cross track error for different static margins

| Static margin | Square pattern | Butterfly pattern |
|----------------|----------------------------------|----------------------------------|
| 2.5% | CT = $1.299 \cdot 10^5$ m (0.95) | CT = $3.469 \cdot 10^5$ m (0.96) |
| 5% | CT = $1.365 \cdot 10^5$ m (1.00) | CT = $3.545 \cdot 10^5$ m (0.98) |
| 7.5% (nominal) | CT = $1.363 \cdot 10^5$ m (1.00) | CT = $3.620 \cdot 10^5$ m (1.00) |
| 10% | CT = $1.436 \cdot 10^5$ m (1.05) | CT = $3.728 \cdot 10^5$ m (1.03) |
| 12% | CT = $1.454 \cdot 10^5$ m (1.07) | CT = $3.927 \cdot 10^5$ m (1.08) |

Fig. 20 2D path for square pattern with different static margins

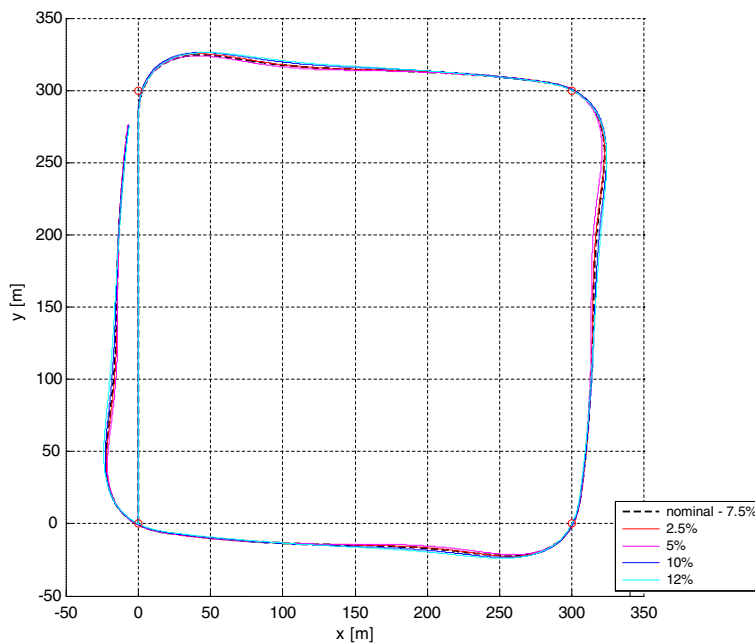


Fig. 21 The trend of the cross track error with different static margins (square pattern)

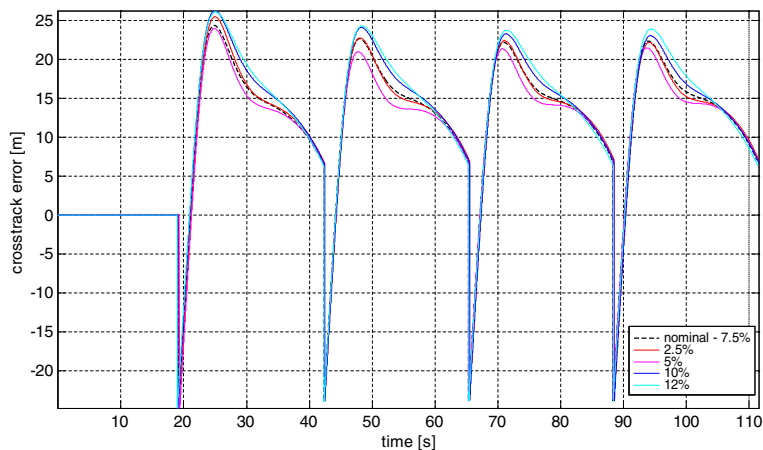


Fig. 22 2D path for butterfly pattern with different static margins

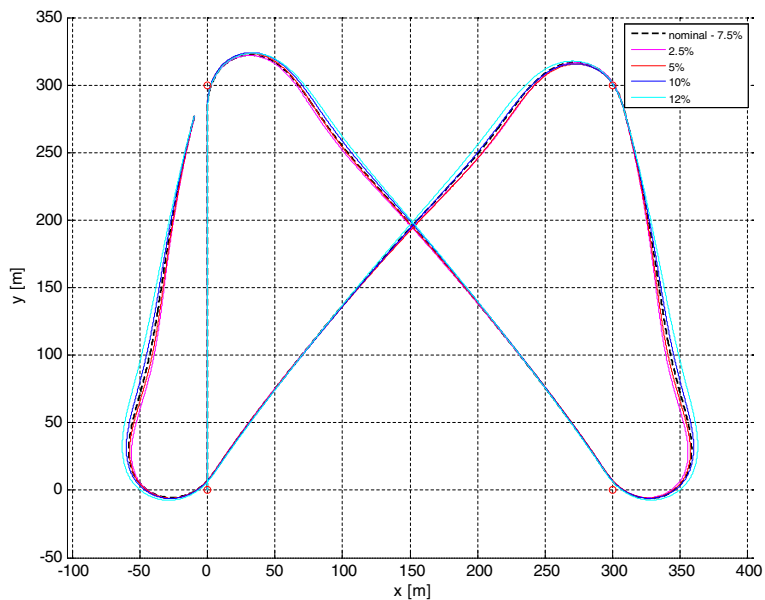


Fig. 23 The trend of the cross track error with different static margins (butterfly pattern)

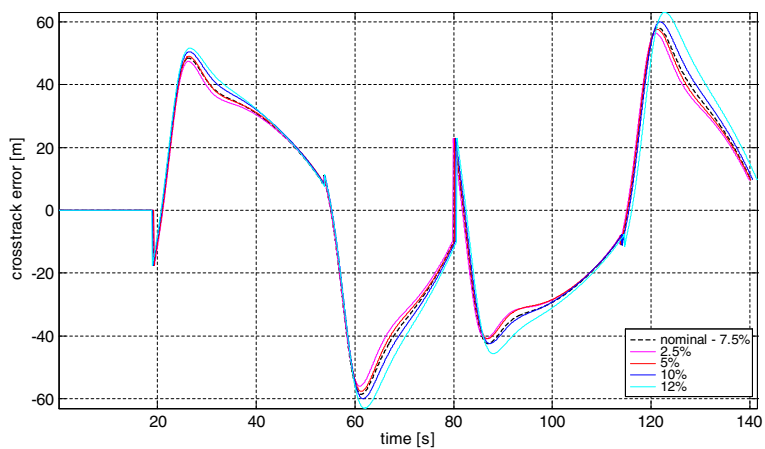


Fig. 24 Elevon deflection with different static margins (square pattern)

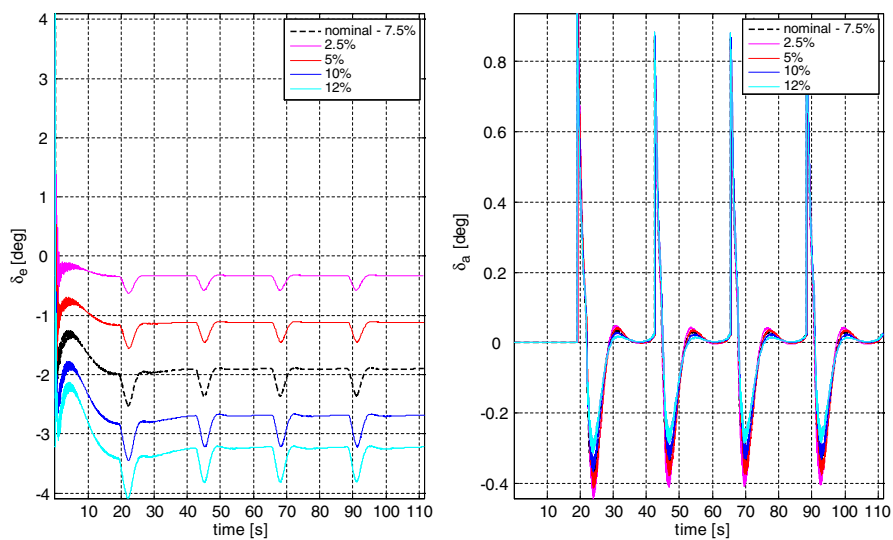
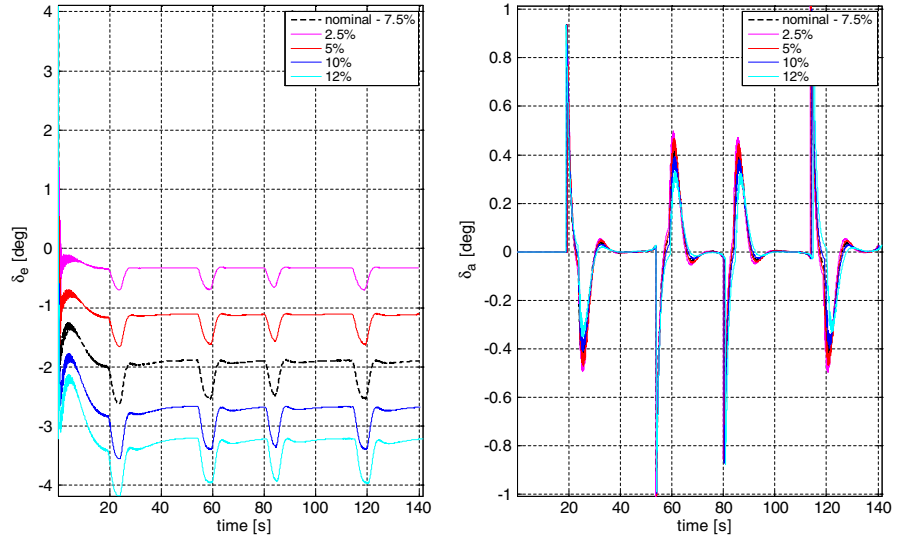


Fig. 25 Elevon deflection with different static margins (butterfly pattern)



During autonomous flight, the vehicle shall respond to attitude, airspeed and altitude errors within the expected accuracy boundaries, as explained in the following section.

Attitude shall be maintained with an accuracy of ± 0.5 deg for pitch angle and ± 1.0 deg for roll angle. In Figs. 13 and in 14 the trend of the pitch and roll angular tracking is drawn, including the effect of the static margin i.e. the location of vehicle's center of gravity. In Figs. 15 and 16 the attitude stabilization and control is verified for the reference case. As evident, the peak of the pitch angle is 8.5 deg, which corresponds with an offset of 1 deg with respect to the reference value. In a similar way, the roll peak is 2 deg lower than the reference value. In both cases the boundaries for tracking error are verified along the complete flight sequence.

The airspeed shall be maintained within $\pm 2\%$ of the reference signal (whichever is greater). In

this case the peak of airspeed correction is about 20% greater than the reference signal (throttle overshoot due to initial transition from climbing to level flight), but the averaged tracking error is kept within the assigned boundary (Fig. 17).

The variation of altitude is compared with the variation of the angle of bank (typical of turning maneuvers), as indicated in [3] and in Table 10. In Fig. 18 the trend is not continuous due to the step time used for the numerical integration.

The typical mission for mini-UAVs is the tracking of assigned waypoints at constant altitude and airspeed. Thus, the minimization of the cross track error (distance off course) and the gradual variations of the control surfaces and, as a consequence, of the flight parameters have to be enforced in flight navigation and control system.

For validation purposes two different patterns are evaluated: a square pattern and a butterfly path (Fig. 19) with a side dimension of 300 m. The

Table 12 Gain scheduling for the aileron-from-roll control loop

| Proportional gain | Derivative gain | Integrative gain |
|-------------------|-----------------|------------------|
| nominal | Nominal | Nominal |
| +25% | Nominal | Nominal |
| +50% | Nominal | Nominal |
| -25% | Nominal | Nominal |
| -50% | Nominal | Nominal |

Table 13 Cumulative cross track error as a function of the aileron-from-roll proportional gain

| Proportional gain (variation) | Square pattern |
|-------------------------------|----------------------------------|
| +25% | CT = $1.382 \cdot 10^5$ m (1.01) |
| +50% | CT = $1.401 \cdot 10^5$ m (1.03) |
| Nominal | CT = $1.363 \cdot 10^5$ m (1.00) |
| -25% | CT = $1.316 \cdot 10^5$ m (0.96) |
| -50% | CT = $1.051 \cdot 10^5$ m (0.77) |

butterfly path revealed to be suitable for exposing potential degradation of the mini-UAV in terms of performance and tracking of the pre-assigned path.

An important setting parameter of the autopilot is the waypoint radius, i.e. when the UAV enters an imaginary circle around a waypoint (radius equal to this parameter) the waypoint is given as “reached” [15]. This parameter is set to 25 m, as a compromise between turn characteristics and gradual correction of the heading during the navigation course towards the next waypoint. Two different flight modes can be also set. With the *fromto* mode the vehicle follows the line/track defined by the points origin and destination while maintaining the current altitude and airspeed (aggressive navigation and control mode that minimizes the cross track error). The second option is the *flyto* mode: this command differs from the *fromto* command in that it makes no attempt to travel in a straight line between two points but keeps the initial heading as a desired state. For the present analysis the less aggressive mode was selected (*flyto*).

The purpose of this analysis is to verify if the mission task is reached minimizing the cross track error with a critical value of the static margin (worst case assessment). Note that the static margin has to be chosen considering the results ob-

tained in terms of dynamic stability (so in terms of flying qualities).

The total cross track error is given in Table 11. This error is the sum of the error evaluated for each time step. The results show that the mission is achieved even if a critical pattern (butterfly) is selected with degraded static margin (compromised longitudinal static stability; Figs. 20, 21, 22, 23).

From these simulations the best results are obtained for the minimum static margin (2.5%) and the cross track error has a peak of ± 20 m. This result does not mean that the aircraft should fly with degraded static and dynamic stability (given as the damping ratio of longitudinal modes). Differently, a vehicle with relaxed static margin is more reactive to control inputs and performs a more aggressive tracking of flight parameters. The correct position of the centre of gravity must be assessed as a compromise of the opposite requirements.

Considering the time domain response of the control surface deflections, gradual variations, compatible with servo excursion, must result even for larger static margins. As evident in Figs. 24 and 25, both the square and the butterfly pattern exhibit similar periodic peaks compatible with range and resolution of actuators.

Another concern is the correct tuning of control loops as a balance between aggressive suppression of tracking errors and minimization of steering

Fig. 26 Elevon deflection with different aileron-from-roll proportional gains (square pattern)

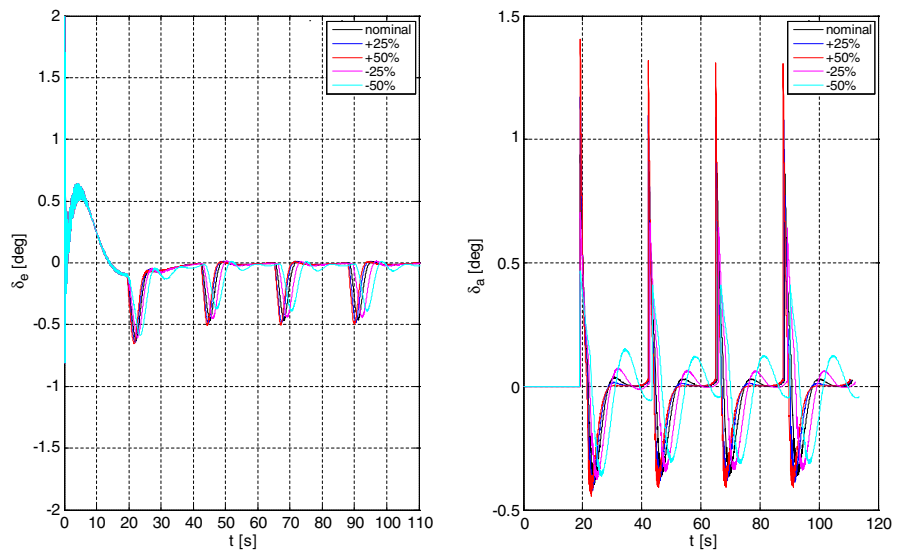


Fig. 27 3D path with different aileron-from-roll proportional gains (square pattern)

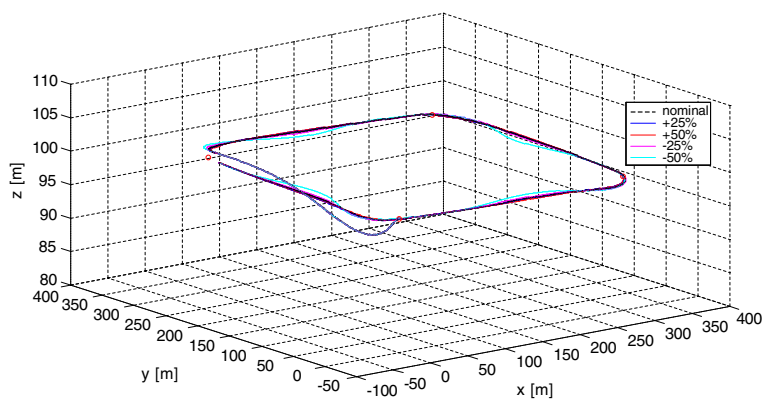


Fig. 28 Elevon deflection with different aileron-from-roll proportional gains (butterfly pattern)

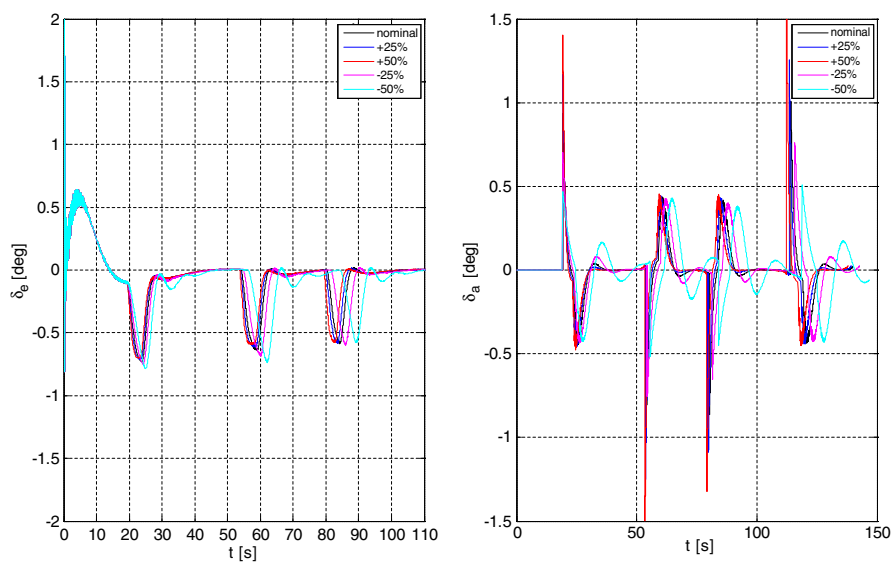


Fig. 29 3D path with different aileron-from-roll proportional gains (butterfly pattern)

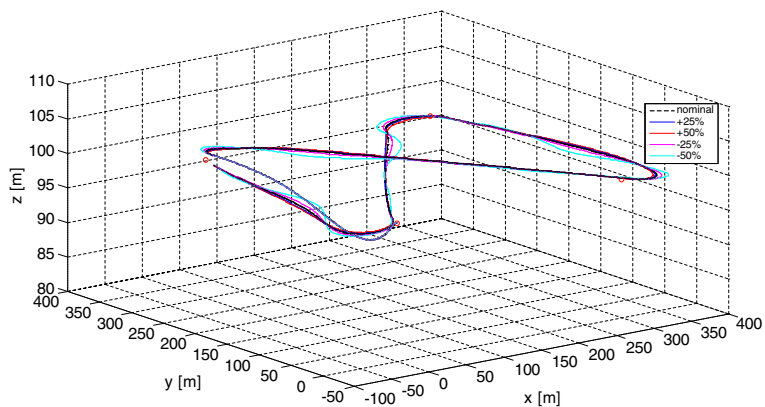


Table 14 Cumulative cross track error as a function of the aileron-from-roll proportional gain (butterfly pattern)

| Proportional gain variation | Butterfly pattern |
|-----------------------------|----------------------------------|
| +25% | CT = $3.632 \cdot 10^5$ m (1.00) |
| +50% | CT = $3.681 \cdot 10^5$ m (1.01) |
| Nominal | CT = $3.621 \cdot 10^5$ m (1.00) |
| -25% | CT = $3.549 \cdot 10^5$ m (0.98) |
| -50% | CT = $3.535 \cdot 10^5$ m (0.97) |

and control losses. Also excessive control compensation (aileron-from-roll in Fig. 12 as an example) may induce an oscillatory response. If the nominal centre of gravity position is considered, the following cases are simulated in Tables 12 and 13.

The nominal gain settings of the control loop were assessed with a trial-and-error procedure, based on empirical loop shaping methods and flight test experiments. The results obtained for the square pattern suggest that, in order to minimize the cross track error, the proportional gain should be decreased (-25%). The simulations performed with the butterfly pattern confirm this conclusion (Figs. 26, 27, 28, 29; Table 14).

In the first seconds of simulation in the altitude variation and in the elevon deflection plot anomalous behavior can be noticed due to the transition between the Pilot in Command (PIC) and the Computer in Command (CIC) modes (start up of the autopilot).

Considering that the process of testing the controller may be expensive and time-consuming, the assessment of gains based on simulations reduces costs and set-up time. If all the control gains (scheme of the autopilot in Fig. 12) are evaluated in this way, the autonomous flight can be optimized with a minimum cross track error and with gradual variations of the surface deflections (i.e. acceptable steering losses). Moreover, with a modal analysis a match between flying and handling qualities can be obtained with excellent vehicle performance and stability.

5 Conclusions and Future Works

The authors propose two different approaches to define flying and handling qualities for mini-UAVs.

Flying qualities are assessed through the modal analysis of longitudinal and lateral-directional dynamics (response oriented approach). The results demonstrate that the manned standards are only partially applicable “as is” to mini-UAVs and the possibility of new type of specifications, starting from mission task elements, is introduced. This preliminary assessment is performed in order to verify the vehicle stability in different flight conditions (in terms of static margins).

The evaluation of handling qualities (presented in Section 4) is performed for autonomous flight mode (task oriented approach) i.e. assigning a sequence of waypoints and flying over a target area. The test vehicle performed the mission task with good ratings, even for reduced longitudinal static stability. As an additional remark, for mini UAVs small external disturbances, i.e. wind and turbulence, can reduce the accuracy of the acquired data during the flight tests. For this reason this simulation-based procedure may significantly reduce the set up time of gain settings for the autopilot.

Future work will address a complete set of flight experiments aiming to reproduce the impact of setting parameters on flight patterns.

References

1. Anonymous: Flying Qualities of Piloted Aircraft MIL-STD-1797 A (1995)
2. Anonymous: Military Specifications, Flying Qualities of Piloted Aircraft MIL-F-8785C (1980)
3. Anonymous: RPV Design Criteria Technical Report AFFDL-TR-76-T25. Rockwell International Cooperation, Columbus, OH (1976)
4. Capello, E., Guglieri, G., Quagliotti, F.: A Software Tool Mission Design and Autopilot Integration: an Application to Micro Aerial Vehicles. EUROSIW. Edinburgh, Scotland (2008)
5. Capello, E., Guglieri, G., Quagliotti, F.: UAVs and Simulation: an experience on MAVs. Aircraft Engineering and Aerospace Technology (2009)
6. Cook, M.: Flight Dynamics Principles. Butterworth Heinemann (2007)
7. Donlan, J.: An Interim Report on the Stability and Control of Tailless airplanes. NACA Technical Report 796 (1944)
8. Foster, T., Bowman, W.: Dynamic Stability and Handling Qualities of Small Unmanned Aerial Vehicles. 43rd AIAA Aerospace Sciences Meeting and Exhibit. Reno, Nevada (2005)

9. Gilruth, R.: Requirements for Satisfactory Flying Qualities of Airplanes. Langley Field, VA: National Advisory Committee for Aeronautics Report 155 (1941)
10. Guglieri, G., Pralio, B., Quagliotti, F.: Flight control system design for a micro aerial vehicle. *Aircraft Eng. Aero. Tech.* **78**, 87–97 (2006)
11. Hodgkinson, J.: *Aircraft Handling Qualities*. AIAA, Washington DC (1999)
12. Holmberg, J., King, D., Leonard, J., Cotting, C.: Flying qualities application and design standards for unmanned air vehicles. Proceedings of 26th Atmospheric Flight Mechanics Conference and Exhibit. Honolulu, Hawaii (2008)
13. Jones, R.: Notes on the Stability and Control of Tailless Airplanes. NACA Technical Report 837 (1941)
14. Marguerettaz, P., Sartori, D., Guglieri, G., Quagliotti, F.: Design and Development of Man-Portable Unmanned Aerial System for Alpine Surveillance Missions. UAS International 2010. Parigi, Francia (2010)
15. Micropilot Inc: Micropilot Autopilot Installation and Operation (2010)
16. Pratt, R.: Flight Control Systems: practical issues in design and implementation. *IEEE Control Engineering Series* 57 (2000)
17. Williams, W.: UAV Handling Qualities... You must be Joking. Aerospace Sciences Cooperation Pty LTd (2003)
18. Williams, W., Harris, M.: The Challenges of Flight Testing Unmanned Air Vehicle. Systems Engineering Test and Evaluation Conference. Sydney, Australia (2002)